P – 03

Depth Encoding of Point-of-Interaction in Thick Scintillation Cameras

Takehiro Tomitani, Yasuyuki Futami, Yasushi Iseki[1], Shigeru Kouda[2], Teiji Nishio[3], Takeshi Murakami, Atsushi Kitagawa, Mitsutaka Kanazawa, Eriko Urakabe, Munefumi Shinbo and Tatsuaki Kanai

Nat. Instit. Rad. Sci., Toshiba Co.[1], Instit. Mole Sci.[2], Nat. Cancer Cent.[3], JAPAN

Introduction

Scintillation cameras[1,2] have been adopted in such field as PET[3,4], positron cameras, focal plane detector for neutron diffraction[5,6], that for angular correlation measurement of annihilation gamma rays and gamma ray astronomy[7]. In our institute, the heavy ion accelerator for heavy ion therapy was built and the secondary beam generator/separator was built last year, from which positron emitting nuclei beams such as ^{10}C, ^{11}C, ^{18}Ne and ^{19}Ne are available. These nuclei emit annihilation pair gamma rays and the distribution of nuclei can be measured with PET or positron camera. We are intending to develop a positron camera dedicated to this objective. In these applications except neutron diffraction, thick NaI(Tl) crystals are adopted to image high energy gamma rays and collimators are not used, which causes two-dimensional(2D) position error that is dependent on the depth of interaction. In principle, depth of interaction can be obtained from the depth-dependency of light distribution. The present study analyzed theoretically the possibility of the detection of depth-of-interaction.

Position Arithmetic

Three-dimensional(3D) position arithmetic can be derived from maximum likelihood estimation[8] by straight forward extension of 2D theory[9,10]. Here we assume that number of photoelectrons generated at photocathode of a photomultiplier (PMT) obeys to Poisson distribution. Photons emitted at position (x, y, z) in the crystal are shared among PMT's. Let n_k denote number of photoelectrons generated at k-th PMT and let $\lambda_k(x, y, z)$ denote its ensemble average. Then the likelihood, L, that m PMT's detect $\{n_1, n_2, ..., n_m\}$ photoelectrons is

$$L(n_1, n_2, ..., n_m|x, y, z) = \prod_{k=1}^{m} p_k(n_k|x, y, z), \tag{1}$$

where p_k, Poisson distribution, is by definition

$$p_k(n_k|x, y, z) = \frac{\lambda_k{}^n}{n!} e^{-\lambda_k}, \tag{2}$$

in which λ_k is a function of the light source position, (x, y, z), however arguments will be omitted for simplicity. A sufficient condition that maximum likelihood estimate (MLE), $(\hat{x}, \hat{y}, \hat{z})$ must satisfy is

$$\frac{\partial \ln L}{\partial x} = 0, \quad \frac{\partial \ln L}{\partial y} = 0 \quad \text{and} \quad \frac{\partial \ln L}{\partial z} = 0. \tag{3}$$

With equations (1) and (2), eq.(3) can be rewritten as

$$q_x(x, y, z) \equiv \frac{\partial \ln L}{\partial x} = \sum_{k=1} \frac{\partial \lambda_k}{\partial x}\left(\frac{n_k}{\lambda_k} - 1\right) = 0,$$

$$q_y(x, y, z) \equiv \frac{\partial \ln L}{\partial y} = \sum_{k=1} \frac{\partial \lambda_k}{\partial y}\left(\frac{n_k}{\lambda_k} - 1\right) = 0,$$

$$q_z(x, y, z) \equiv \frac{\partial \ln L}{\partial z} = \sum_{k=1} \frac{\partial \lambda_k}{\partial z}\left(\frac{n_k}{\lambda_k} - 1\right) = 0. \tag{4}$$

MLE, $(\hat{x}, \hat{y}, \hat{z})$, is determined from this set of equations. Note that each equation is implicitly dependent on x, y and z through $\lambda(x, y, z)$ and transcendental and hence can only be solved numerically. To this end, Newton-Raphson's approximation works, which is an extension of Newtown's approximation method to multi-parameter equations. It adopts iterative procedure starting from some initial guess and from k-th approximate solutions, (x_k, y_k, z_k), we seek for the next approximation, $x_{k+1}=x_k+\xi$, $y_{k+1}=y_k+\psi$, $z_{k+1}= z_k+\zeta$ by retaining the first order terms of Taylor expansions.

$$q_x(x_{k+1}, y_{k+1}, z_{k+1}) \approx q_x(x_k, y_k, z_k) + \frac{\partial q_x}{\partial x}\xi + \frac{\partial q_x}{\partial y}\psi + \frac{\partial q_x}{\partial z}\zeta \approx 0,$$

$$q_y(x_{k+1}, y_{k+1}, z_{k+1}) \approx q_y(x_k, y_k, z_k) + \frac{\partial q_y}{\partial x}\xi + \frac{\partial q_y}{\partial y}\psi + \frac{\partial q_y}{\partial z}\zeta \approx 0,$$

$$q_z(x_{k+1}, y_{k+1}, z_{k+1}) \approx q_z(x_k, y_k, z_k) + \frac{\partial q_z}{\partial x}\xi + \frac{\partial q_z}{\partial y}\psi + \frac{\partial q_z}{\partial z}\zeta \approx 0. \tag{5}$$

Solving this set of equations, we have

$$\xi = |-\mathbf{q}, \mathbf{q_y}, \mathbf{q_z}|\, D^{-1}, \quad \psi = |\mathbf{q_x}, -\mathbf{q}, \mathbf{q_z}|\, D^{-1}, \quad \zeta = |\mathbf{q_x}, \mathbf{q_y}, -\mathbf{q}|\, D^{-1}, \tag{6}$$

where $\mathbf{q} = (q_x, q_y, q_z)^T$, $\mathbf{q_x} = \dfrac{\partial \mathbf{q}}{\partial x}$, $\mathbf{q_y} = \dfrac{\partial \mathbf{q}}{\partial y}$, $\mathbf{q_z} = \dfrac{\partial \mathbf{q}}{\partial z}$ and $D = |\mathbf{q_x}, \mathbf{q_y}, \mathbf{q_z}|$.

This procedure takes time so that it can only be realized if all PMT intensity data are stored digitally and the event rate is low. In our case, activity level is quite low and the counting rate is at most some hundreds cps so that this approach is feasible.

Fisher's Information and Covariance Matrix

Fisher introduced a matrix that describes the amount of information available in the system[8]. According to Fisher, the information matrix, **J**, is defined as

$$\mathbf{J} \equiv E\left[(\nabla \ln L)^T (\nabla \ln L)\right] = E\left[\nabla^T \nabla \ln L\right], \quad \nabla \equiv (\partial/\partial x, \partial/\partial y, \partial/\partial x) \tag{7}$$

in which $(\cdot)^T$ represents matrix transpose. Elements of **J** are calculated as

$$J_{xx} = \sum_{k=1} \frac{1}{\lambda_k}\left(\frac{\partial \lambda_k}{\partial x}\right)^2, \quad J_{yy} = \sum_{k=1} \frac{1}{\lambda_k}\left(\frac{\partial \lambda_k}{\partial y}\right)^2, \quad J_{zz} = \sum_{k=1} \frac{1}{\lambda_k}\left(\frac{\partial \lambda_k}{\partial z}\right)^2,$$

$$J_{zy} = J_{yz} = \sum_{i=1} \frac{1}{\lambda_i}\frac{\partial \lambda_i}{\partial y}\frac{\partial \lambda_i}{\partial z}, \quad J_{xz} = J_{zx} = \sum_{i=1} \frac{1}{\lambda_i}\frac{\partial \lambda_i}{\partial x}\frac{\partial \lambda_i}{\partial z}, \quad J_{yx} = J_{xy} = \sum_{i=1} \frac{1}{\lambda_i}\frac{\partial \lambda_i}{\partial x}\frac{\partial \lambda_i}{\partial y}, \tag{8}$$

Covariance matrix, **V**, of the estimate, $(\hat{x}, \hat{y}, \hat{z})$, is equal to the matrix inverse of **J**, i. e., $\mathbf{V} = \mathbf{J}^{-1}$.[8] We can calculate the spatial resolutions from its diagonal components.

Light Reflection

Depth-resolution is solely dependent on the dependency of light distribution, that is strongly dependent on the way of reflection on the surface opposite to PMT array. In the case of perfect diffusive reflection, we first performed Monte Carlo simulations of light transport and the resultant light distributions was fitted to Cauchy's distribution within limited error.

$$f(x, y, z) = \frac{\omega(z)^2}{x^2 + y^2 + \omega(z)^2} \tag{9}$$

The dispersions, $\omega(z)$, of Cauchy's distributions are plotted as a function of depth in left side of Fig. 1. The distribution has a broad maximum near the surface and the estimate of depth may be divalent and not unique and so the depth cannot be determined.

In the case of mirror reflection, distribution of reflected light is equal to that of the mirror image

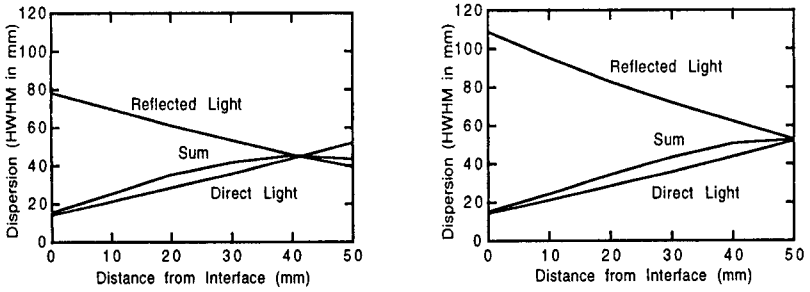

Fig. 1. Dispersions of light distribution as a function of depth of interaction in the case of perfectly diffusive reflection(left) and that of mirror reflection(right).

of light source, so that the distribution of total light is symmetric with respect to the mirror surface and its derivative is zero as can be seen in the right side graph of Fig. 1, which implies no depth information is available at the surface. Solid angle subtended by a square PMT is

$$\Omega(x, y, z) = \int_{-s}^{+s} \int_{-s}^{+s} \frac{z\, du\, dv}{\left[(x-u)^2 + (y-v)^2 + z^2\right]^{3/2}}$$

$$= 4\pi \tan^{-1}\left[\frac{(u-x)(v-y)}{z\sqrt{(u-x)^2 + (v-y)^2 + z^2}}\right] \Bigg|_{u=-s}^{u=+s} \Bigg|_{u=-s}^{u=+s}, \qquad (10)$$

where (x, y, z) and (u, v) denote the position of light source and 2D position on the PMT surface, respectively. In the case of circular PMT, solid angle can be expressed by Jacobi's elliptic integral of the third kind. The latter expression is more complex and so the former model was adopted in the present analyses because of simplicity. The present analyses deal with mirror reflection, half-opaque and opaque reflections. The PMT configuration is shown in Fig. 2.

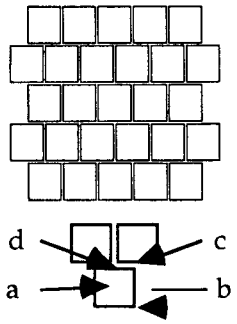

Fig. 2. PMT configuration of the PMT's of square cross-section. A sketch below shows points of interests on which spatial resolutions were calculated.

Spatial Resolution

3D spatial resolutions in the case of mirror reflection are shown in the left column of Fig. 3. The opposite extreme is the opaque surface in which light is absorbed at the surface and some 2D spatial information is lost. 3D spatial resolutions are plotted in the right column of Fig. 3. Inbetween is the case of half-opaque surface, in which some fractions of light are absorbed at the reflection surface. 3D spatial resolutions of semi-opaque case are inbetween as shown in the middle column of Fig. 3.

Discussions and Conclusions

In view of 2D position arithmetic, perfectly diffusive reflection is superior to mirro reflection, yet depth information cannot be derived. Depth information can be obtained in the case of mirror reflection with reflection coefficient ranging from 0 to 1, that is, opaque to mirror reflection. From Fig. 3, one can conclude that depth resolution can be obtained at a cost of 2-D spatial resolution. The choice seems dependent on the purposes of particular applications. In the case of parallax correction, only moderate depth information may suffice, while in other cases such as gamma ray astronomy, depth information may be more important to determine the gamma ray direction.

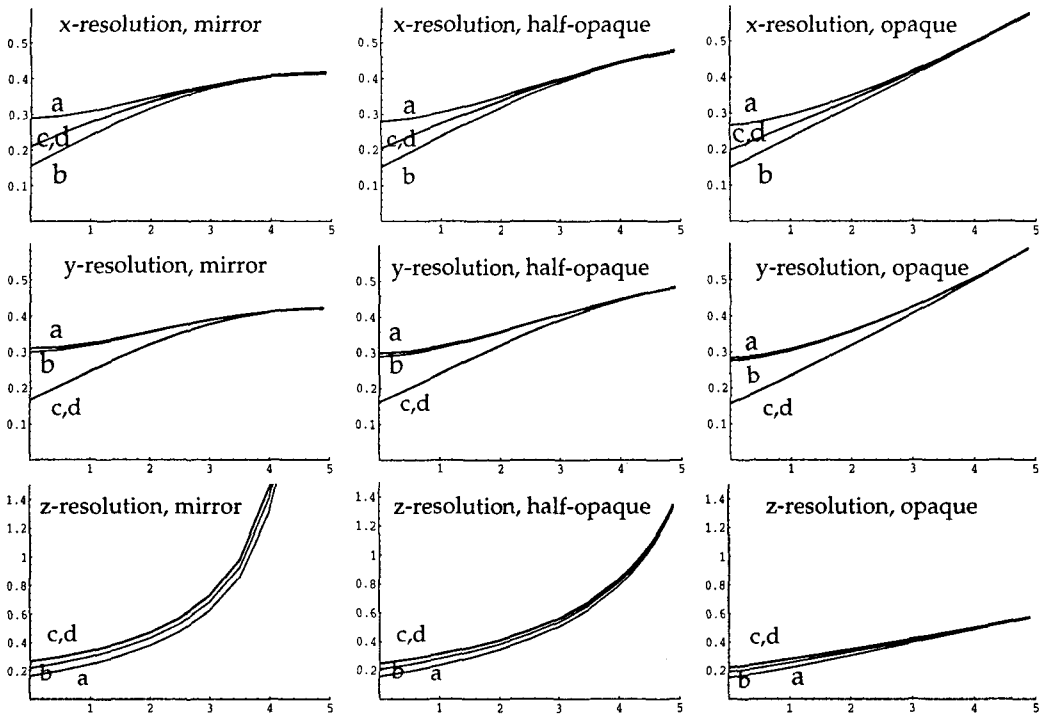

Fig. 3. Spatial resolutions as a function of depth of light source. Ordinate is spatial resolution in cm FWHM and abscissa is depth in cm. Curves a, b, c and d refer to the positions shown in fig. 2.

References

1. H. O. Anger, "Scintillation Camera." Rev. Sci. Instr. **29**: 27-33, 1958.
2. E. Tanaka, T. Hiramotor, et al. . "Scintillation cameras based on new position arithmetic." J. Nucl. Med. **11**: 542-547, 1970.
3. J. S. Karp and G. Muehlehner, "Performance of a position-sensitive scintillation detector." Phys. Med. Biol. **30**: 643-655, 1985.
4. J. S. Karp, D.A.Mankoff et al., "A position-sensitive detector for use in positron emission tomography." Nucl. Instr. Meth. **A273**: 891-897, 1988.
5. M. G. Strauss, R. Brenner et al., "2-D position sensitive scintillation detector for neutrons." IEEE Trans. Nucl. Sci. **NS-28**: 800-806, 1981.
6. R. Kurz, I. Naday et al., "One- and two-dimensional position sensitive scintillation detectors for thermal neutrons." IEEE Trans. Nucl. Sci. **NS-32**: 453-456, 1985.
7. W. R. Cook, M. Finger et al., "A thick Anger camera for gamma-ray astronomy." IEEE Trans. Nucl. Sci. **NS-32**: 129-133, 1985.
8. M. G. Kendall and A. Stuart, The Advanced Theory of Statistics, Vol. 2, "Inference and Relationship": Charles Griffin & Company Ltd., 1961, pp. 35-97.
9. R. M. Gray and A. Macovski, "Maximum a posteriori estimation of position in scintillation cameras." IEEE Tran. Nucl. Sci. **NS-23**: 849-852, 1976.
10. S. Degerine and M. Laval, "Statistical study of a gamma camera transfer function," **22**:760-768, 1977.